# Supporting Information

## Gasson et al. 10.1073/pnas.1516130113

### Climate–Ice Sheet Feedbacks

As an ice sheet changes because of climate forcing, the ice sheet can subsequently alter the surface climate, creating a feedback. This effect is attributable to changes in elevation, surface albedo, and large-scale circulation (37, 38). The effects of changes in elevation on surface mass balance are often accounted for by using a lapse-rate correction for temperature (a similar correction can be applied to precipitation); however, other climate feedbacks are often neglected. The difficulty of including all climate feedbacks is partially attributable to the different response times of the ice sheets ($10^3$–$10^5$ y) and the climate system (days to $10^3$ y) and the significant computational expense of running climate models. Recent work has used a matrix of climate simulations from a GCM to account for ice sheet–climate feedbacks, by interpolating between different GCM simulations with varying ice sheet extent (37). However, a major drawback of this approach is that the interpolation is based on total ice sheet area within the domain; as such, the climate feedback is averaged over the whole domain. Another approach is to use an asynchronously coupled GCM whereby the climate model and ice sheet model are periodically coupled (66) or a full coupling with a reduced complexity climate model (67). However, the coarse resolution of these climate models may not be able to fully resolve the narrow Antarctic ablation zone that develops in warmer climate simulations parallel to the ice margin. This coarse resolution is a particular problem when there is ice sheet retreat into relatively narrow glacier channels, which may be below the resolution of the climate model. To improve simulation of ice sheet–climate feedbacks, we use a high-resolution regional climate model that is periodically coupled to the ice sheet model to account for these feedbacks (also see Fig. 1). Because the climate model is of lower resolution than the ice sheet model, a lapse-rate temperature correction is also made to account for any discrepancies in the surface elevation between the climate model and the ice sheet model.

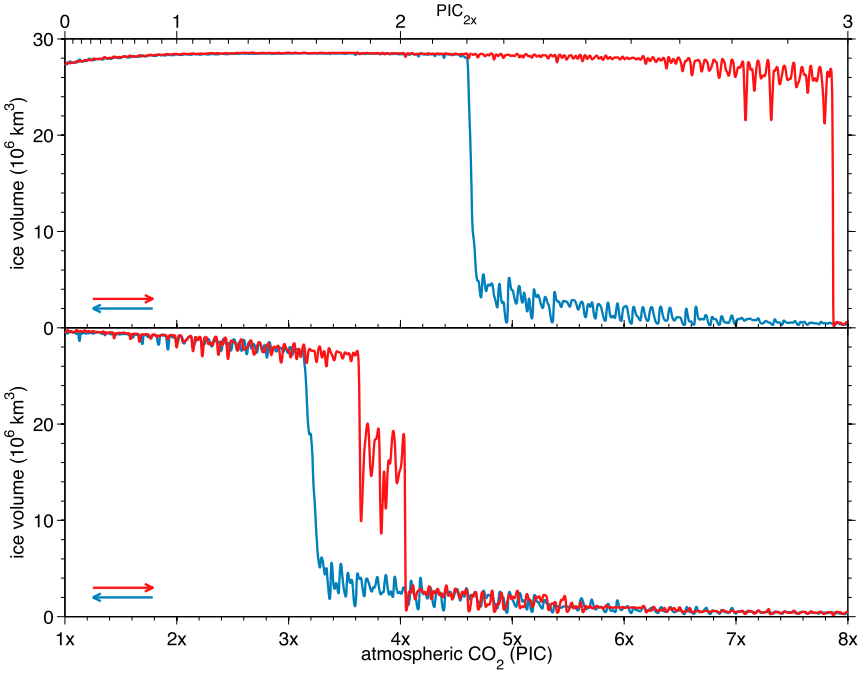


**Fig. S1.** Earlier simulations of Antarctic glaciation/deglaciation by linearly increasing/decreasing atmospheric $CO_2$, with astronomical variability included, which causes the higher frequency noise. Atmospheric $CO_2$ is shown as multiples of preindustrial concentrations (PIC). Climate forcing comes from the GCM matrix method, outlined in ref. 37, using a matrix of 18 GCM simulations, with different astronomical configuration, atmospheric $CO_2$, and Antarctic ice sheet extent. (*Upper*) Includes a representation of albedo feedback by scaling between GCM simulations with different Antarctic ice sheet extent, based on the total ice area in the ice sheet model domain. (*Lower*) Excludes albedo feedback; here, the hysteresis is caused solely by height–mass balance feedback. Simulations are from ref. 68, which includes a full description of the methodology; note that these simulations do not include any marine instabilities.

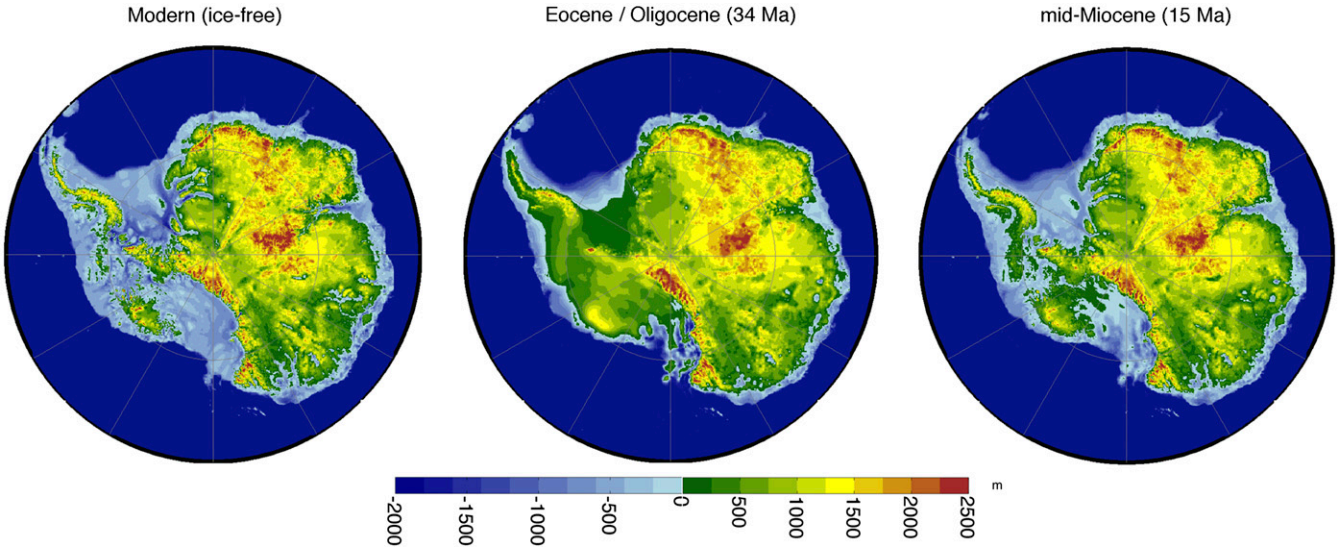


**Fig. S2.** Different Antarctic bedrock topographies used. (*Left*) The modern Bedmap2 topography (33) following the removal of the ice sheet and adjustment for isostatic rebound; data from ref. 42. (*Center*) Eocene/Oligocene "maximum" reconstruction; data from ref. 40. Note the greater extent of West Antarctic land above sea level in this reconstruction. (*Right*) The mid-Miocene reconstruction, created by scaling linearly between the modern Bedmap2 dataset and the Eocene/Oligocene reconstruction.

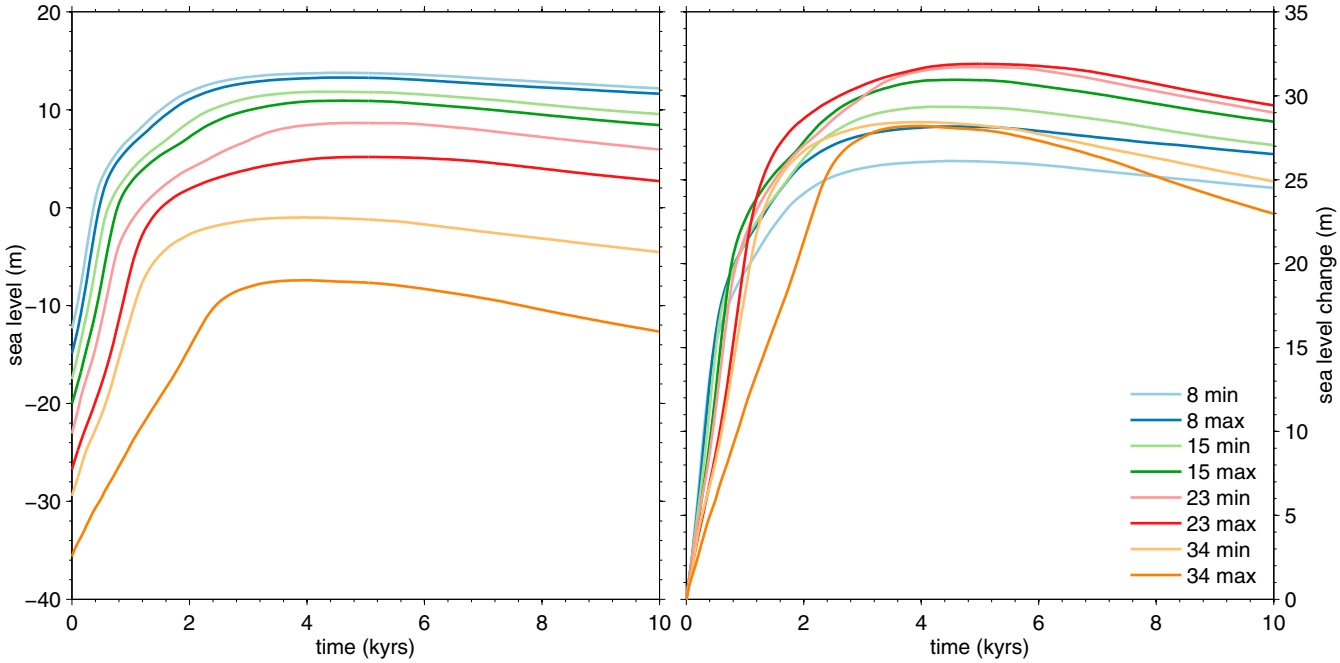


**Fig. S3.** Sensitivity of model to bedrock topography for instantaneous warming experiments (warmer climate forcing, 500-ppm $CO_2$, no climate feedbacks). Note the increased initial ice volume for the older topographies, which are more similar to the Eocene/Oligocene topography of ref. 40 and have a greater area of land above sea level, particularly in the West Antarctic. Despite the large difference in response, the change in sea level is similar for all topographies. "max" and "min" are scaled between either the Eocene–Oligocene maximum or minimum reconstructions of ref. 40.

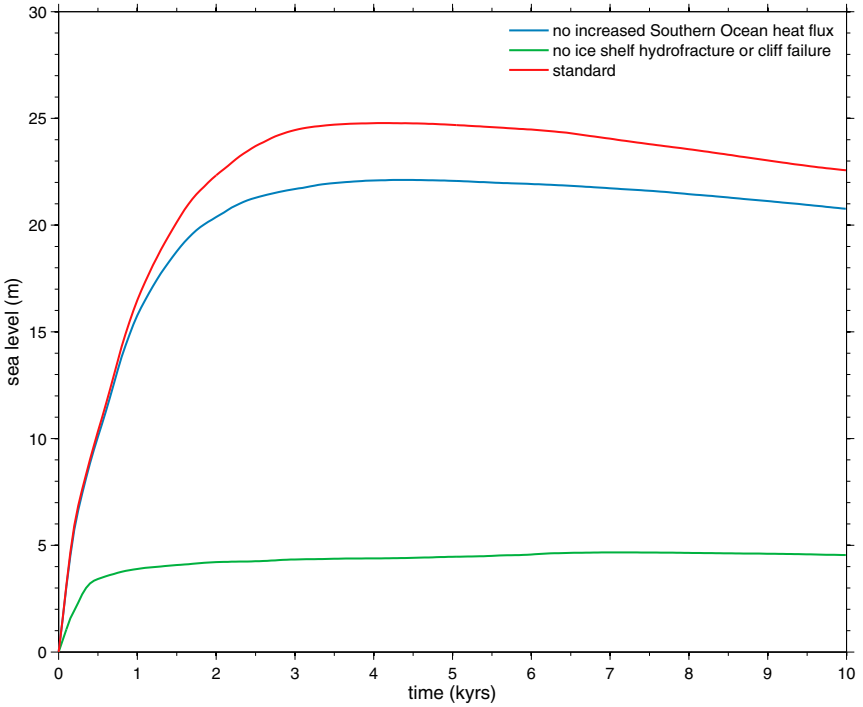


**Fig. S4.** Sensitivity tests, showing impact of increase heat flux into the Southern Ocean (63), specified in all "warmer" climate simulations. Also shown are simulations without ice-shelf hydrofracture or ice-cliff failure. Instantaneous warming experiments (from cold climate forcing to warmer climate forcing with 500-ppm $CO_2$) performed on modern Bedmap2 topography and are without climate feedback.

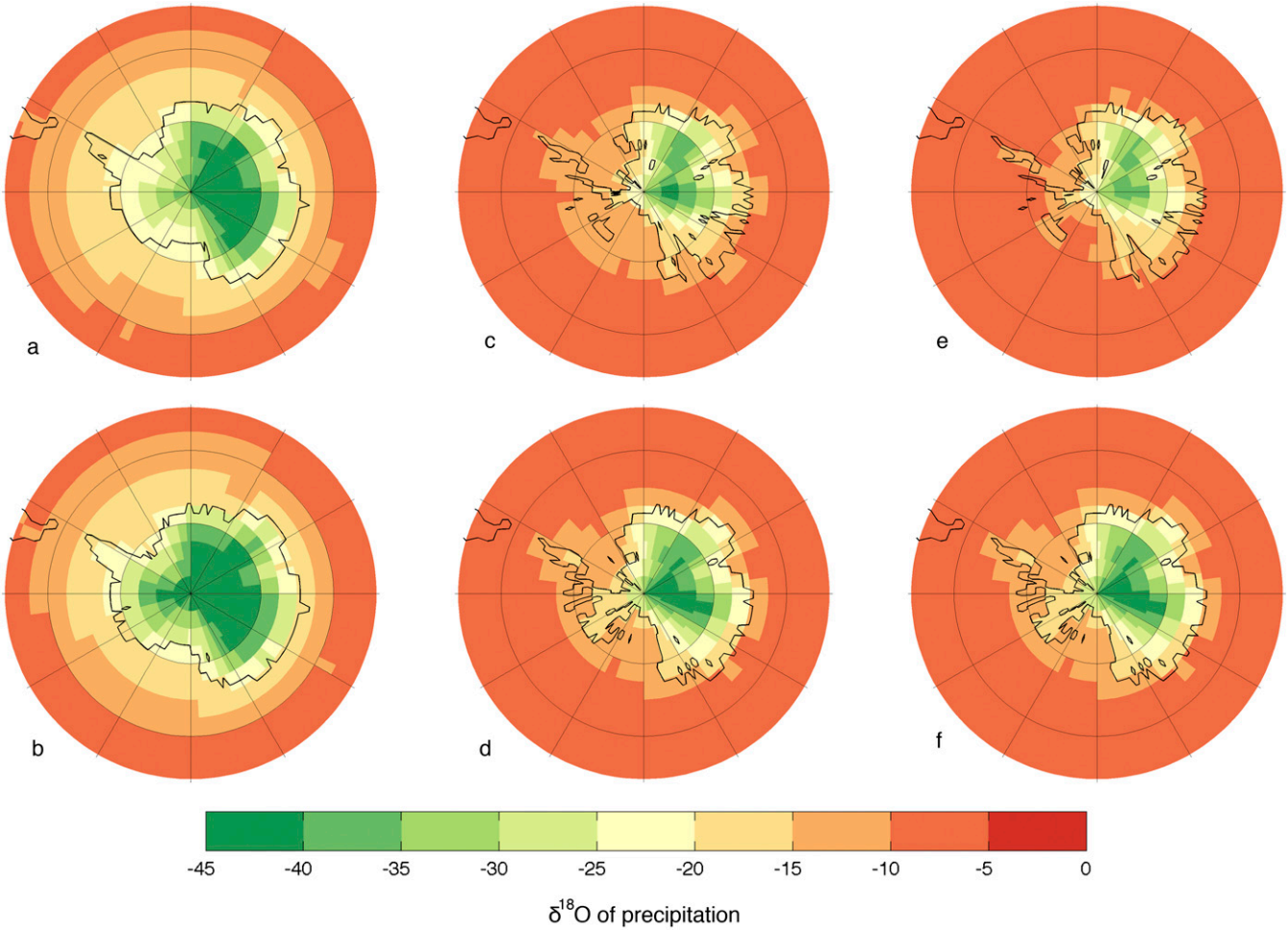


**Fig. S5.** GCM output showing $\delta^{18}O$ of precipitation (‰). The upper row uses modern Antarctic topography (*A*, *C*, and *E*) (Scenario A), and the lower row uses mid-Miocene topography (*B*, *D*, and *F*) (Scenario B); paleogeography for the rest of the globe is for the mid-Miocene for all simulations. (*A* and *B*) Colder climate (atmospheric $CO_2$, 280 ppm). (*C* and *D*) Warmer climate (atmospheric $CO_2$, 500 ppm). (*E* and *F*) High $CO_2$ experiment (atmospheric $CO_2$, 840 ppm).

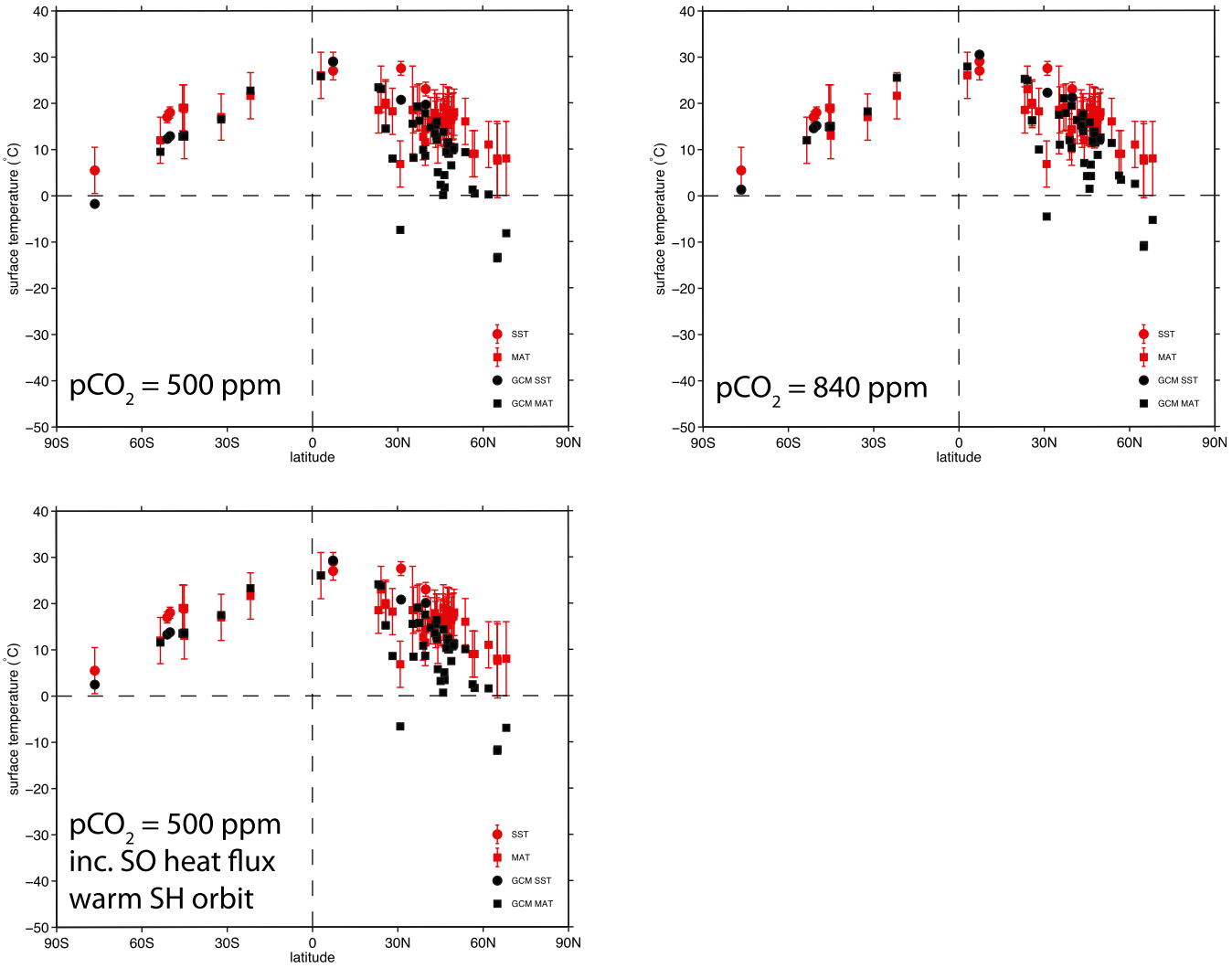


**Fig. S6.** GCM–proxy data comparison of sea surface temperature and mean air temperature data for the middle Miocene climatic optimum. Proxy compilation is from ref. 54; see the original reference for details of data used. Simulations are for 500 ppm (*Upper Left*) and 840 ppm (*Upper Right*) $CO_2$ simulations with a mean "modern" astronomical configuration; only the 840-ppm simulation is within error of the high-latitude southern hemisphere proxy data. (*Lower*) Also shown is a simulation with 500-ppm $CO_2$, a "warm" austral summer astronomical configuration and a small increase (inc.) in the Southern Ocean (SO) heat flux, following the methodology of ref. 63.